

Colloidal Transition-Metal-Doped ZnO Quantum Dots

Pavle V. Radovanovic, Nick S. Norberg, Kathryn E. McNally, and Daniel R. Gamelin*

Department of Chemistry, Box 351700, University of Washington, Seattle, Washington 98195-1700

Received September 4, 2002

Methods for introducing new magnetic, optical, electronic, photophysical, or photochemical properties to semiconductor nanocrystals are attracting intense interest as prospects for nanotechnological applications emerge in the areas of spintronics,¹ optoelectronics,^{2,3} quantum computing,⁴ photocatalysis,⁵ and luminescence labeling.⁶ An effective method for manipulating the physical properties of semiconductors involves impurity doping. A great deal of attention has been paid to doping bulk semiconductors with magnetic ions such as Mn^{2+} to impart the unusual giant Zeeman, Faraday rotation, and magnetic polaron effects that characterize this class of materials, known as diluted magnetic semiconductors (DMSs).⁷ Advances in vacuum-deposition methods have allowed preparation of many new nanoscale DMSs that have shown unique magnetic, magneto-optical, and magnetoelectronic properties.^{2,3,8,9} These successes have motivated us to develop solution-based synthetic routes for preparation of high-quality colloidal DMS quantum dots (DMS-QDs).¹⁰ The solution compatibility and chemical flexibility of colloidal semiconductor nanocrystals allow them to be easily incorporated into glasses or polymers, appended to biomolecules, or assembled into close-packed ordered arrays, providing many opportunities related to materials processing and nanoscale engineering.

To date, solution synthesis of free-standing high-quality DMS-QDs has been limited to II–VI chalcogenides (CdS, CdSe, ZnS, and ZnSe).^{10–12} Access to a wider variety of colloidal doped QDs would substantially increase the range of possible nanotechnological applications. ZnO is an attractive semiconductor for numerous applications because of its hardness, chemical stability, optical transparency, large exciton binding energy, and piezoelectric properties.¹³ ZnO DMS thin films have recently been prepared by vacuum-deposition methods that show large magneto-optical effects and the promise of high- T_C ferromagnetism.⁹ In this communication we report the preparation and electronic absorption spectroscopy of colloidal ZnO DMS-QDs. Our procedure¹⁴ for synthesizing transition-metal-doped ZnO QDs is adapted from literature methods known to yield highly crystalline and relatively monodisperse nanocrystals of pure ZnO.¹⁵ A major concern in the preparation of DMS nanocrystals from solution is dopant extrusion during growth,^{3,10,12} which may compromise the desired physical properties. We use ligand-field electronic absorption spectroscopy as a dopant-specific optical probe¹⁰ to monitor incorporation during nanocrystal growth and to verify internal substitutional doping in Co^{2+} :ZnO and Ni^{2+} :ZnO DMS-QDs.

Figure 1 shows a series of ligand-field electronic absorption spectra collected in situ during the synthesis of Co^{2+} :ZnO QDs.¹⁴ In the quantum-confined size regime (diameter $\leq \sim 7$ nm for ZnO) nanocrystal growth is accompanied by band gap reduction.¹⁵ Also accompanying nanocrystal growth is the appearance of a structured absorption feature centered at $16\,500\text{ cm}^{-1}$ associated with the

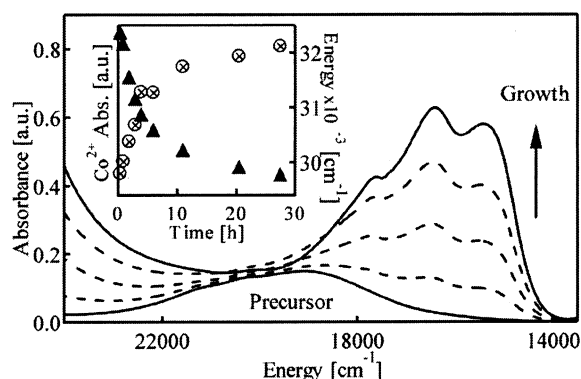


Figure 1. 300 K absorption of Co^{2+} :ZnO DMS-QDs during synthesis. With nanocrystal growth, Co^{2+} converts from octahedral (${}^4T_{1g}(F) \rightarrow {}^4T_{1g}(P)$, $19\,500\text{ cm}^{-1}$) to tetrahedral (${}^4A_2 \rightarrow {}^4T_1(P)$, $16\,500\text{ cm}^{-1}$) geometry. Inset: Tetrahedral Co^{2+} absorbance at $15\,500\text{ cm}^{-1}$ (\otimes) and ZnO band gap energy (\blacktriangle) vs time.

spin–orbit split ${}^4A_2 \rightarrow {}^4T_1(P)$ ligand-field transition of tetrahedral Co^{2+} .¹⁶ From its similarity to that of bulk Co^{2+} :ZnO,¹⁷ we conclude that the tetrahedral absorption signal in Figure 1 arises predominantly from Co^{2+} ions that are substitutionally doped at Zn^{2+} sites of the ZnO nanocrystals (vide infra). The inset of Figure 1 plots the increase in tetrahedral Co^{2+} ${}^4A_2 \rightarrow {}^4T_1(P)$ absorption intensity and the decrease in ZnO band gap energy measured as a function of time during nanocrystal growth, and demonstrates that tetrahedral Co^{2+} is formed concurrently with nanocrystal growth. Collectively, the data of Figure 1 provide strong evidence that Co^{2+} is isotropically doped throughout the ZnO nanocrystals. Isotropic substitutional doping was also observed in the synthesis of Co^{2+} :ZnS DMS-QDs from solution,¹⁰ and in both lattices it is attributed to the compatible tetrahedral ionic radii of Co^{2+} and Zn^{2+} (both ca. 0.71 \AA).

Even in the isotropic limit, many dopants are expected to reside on the nanocrystal surfaces due to their high surface-to-volume ratios. Completely internally doped Co^{2+} :ZnO DMS-QDs can be prepared by the isocrystalline core/shell (ICS) procedure,¹⁰ in which washed as-prepared nanocrystals are treated with alternating additions of Zn^{2+} and OH^- , encapsulating any surface-bound dopants under a ZnO epitaxial shell. Upon shell growth, the ligand-field band narrows slightly and its high-energy tail is diminished (Supporting Information). The resulting spectrum (Figure 2a) is essentially identical to that of bulk $\sim 0.1\%$ Co^{2+} :ZnO (Figure 2b).¹⁷ These subtle changes are attributed to internalization of a minor population of surface-bound Co^{2+} ions, which likely have terminal hydroxide or acetate ligation in the as-prepared sample. These conclusions are supported by deliberate binding of Co^{2+} to the surfaces of undoped ZnO QDs, followed by washing and resuspension, which yields a broad higher-energy spectrum (Figure 2c) distinctly different from that of Figure 2a and similar to that of $[Co(OH)_4]^{2-}$.¹⁶ Growth of a ZnO shell in this case again yields the

* To whom correspondence should be addressed. E-mail: gamelin@chem.washington.edu.

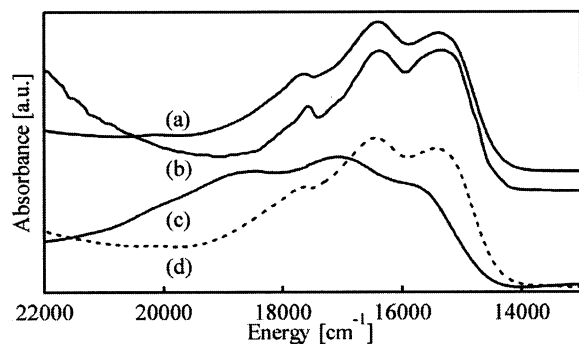


Figure 2. 300 K $\text{Co}^{2+} {}^4\text{A}_2 \rightarrow {}^4\text{T}_1(\text{P})$ ligand-field absorption of (a) isocrystalline core/shell $\text{Co}^{2+}:\text{ZnO}$ QDs in EtOH, (b) bulk $\text{Co}^{2+}:\text{ZnO}$ single crystal (ref 17), (c) ZnO QDs in EtOH with Co^{2+} deliberately surface-bound, and (d) sample (c) following isocrystalline shell growth.

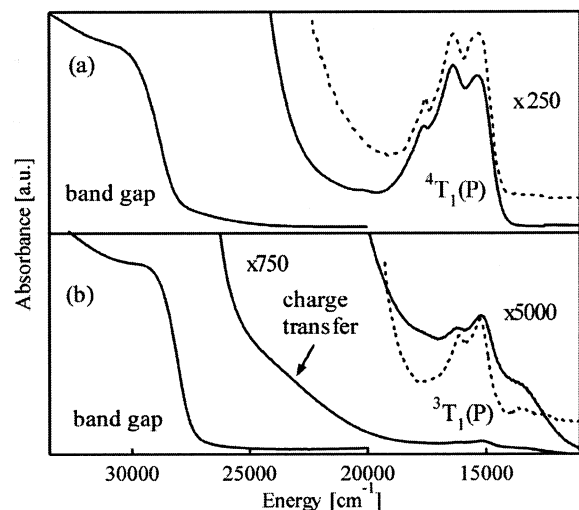


Figure 3. Overview 300 K electronic absorption spectra of EtOH colloid solutions of (a) 4.0 nm 4.3% $\text{Co}^{2+}:\text{ZnO}$ QDs and (b) 4.5 nm 0.2% $\text{Ni}^{2+}:\text{ZnO}$ QDs. Bulk single-crystal spectra of $\sim 0.1\%$ $\text{Co}^{2+}:\text{ZnO}$ and $\sim 0.1\%$ $\text{Ni}^{2+}:\text{ZnO}$ (dashed, ref 17) are included for comparison.

spectrum of internally doped Co^{2+} (Figure 2d), verifying the efficacy of this procedure in internalizing surface-bound dopants. From the data in Figures 1 and 2 we conclude that $\text{Co}^{2+}:\text{ZnO}$ QDs prepared by the ICS procedure are isotropically doped within their cores and that doping involves substitution at the Zn^{2+} lattice sites. An overview absorption spectrum of 4.0 nm 4.3% $\text{Co}^{2+}:\text{ZnO}$ QDs prepared by the ICS procedure is shown in Figure 3a.

This procedure is general and can be applied with other dopant ions. Figure 3b shows an overview absorption spectrum of 4.5 nm 0.2% $\text{Ni}^{2+}:\text{ZnO}$ DMS-QDs prepared by the ICS procedure. The ligand-field energies are essentially identical to those of bulk $\text{Ni}^{2+}:\text{ZnO}$,¹⁷ confirming substitutional core doping. The broad shoulder at $24\,000\text{ cm}^{-1}$ has been assigned in bulk as an oxide-to- Ni^{2+} LMCT transition.¹⁷ The appearance of a sub-bandgap LMCT transition in $\text{Ni}^{2+}:\text{ZnO}$ and not in $\text{Co}^{2+}:\text{ZnO}$ reflects the greater electronegativity of Ni^{2+} . Analogous LMCT transitions have been shown to sensitize photoredox chemistry in related microcrystalline Ni^{2+} -doped semiconductor photocatalysts.⁵ The colloidal core-doped $\text{Ni}^{2+}:\text{ZnO}$ nanocrystals of Figure 3b offer the unique combination of extremely high surface areas and homogeneous Ni^{2+} speciation,

and their study may lead to a deeper mechanistic understanding of photosensitization in this class of materials.

In summary, high-quality colloidal transition-metal-doped ZnO quantum dots have been synthesized. To our knowledge, these are the first free-standing oxide DMS-QDs reported. The synthesis of colloidal oxide DMS-QDs introduces a new category of magnetic semiconductor materials available for physical study and application in nanotechnology. The magnetic properties of these materials are currently under investigation.

Acknowledgment. This research was supported by The Petroleum Research Fund, Research Corporation, the UW, and its Center for Nanotechnology. P.V.R. thanks the UW Center for Nanotechnology and N.S.N. thanks the UW/PNNL Joint Institutes for Nanotechnology for Graduate Research Awards.

Supporting Information Available: Representative powder XRD, HRTEM, selected area diffraction, and absorption data (PDF). This material is available free of charge via the Internet at <http://pubs.acs.org>.

References

- (1) Wolf, S. A.; Awschalom, D. D.; Buhrman, R. A.; Daughton, J. M.; von Molnár, S.; Roukes, M. L.; Chhelkanova, A. Y.; Treger, D. M. *Science* **2001**, *294*, 1488.
- (2) Ando, K. In *Solid-State Sciences: Magneto-Optics*; Springer: 2000; Vol. 128; p 211.
- (3) Shim, M.; Wang, C.; Norris, D. J.; Guyot-Sionnest, P. *MRS Bull.* **2001**, *26*, 1005.
- (4) Golovach, V. N.; Loss, D. *Semicond. Sci. Technol.* **2002**, *17*, 355.
- (5) Kudo, A.; Sekizawa, M. *Chem. Commun.* **2000**, 1371. Zou, Z.; Ye, J.; Sayama, K.; Arakawa, H. *Nature* **2001**, *414*, 625.
- (6) Chan, W. C. W.; Nie, S. *Science* **1998**, *281*, 2016. Bruchez, M., Jr.; Moronne, M.; Gin, P.; Weiss, S.; Alivisatos, A. P. *Science* **1998**, *281*, 2013.
- (7) *Semiconductors and Semimetals*; Willardson, R. K., Beer, A. C., Eds.; Diluted Magnetic Semiconductors; Furdyna, J. K., Kossut, J., Eds.; Vol. 25; Academic: New York, 1988.
- (8) Matsumoto, Y.; Murakami, M.; Shono, T.; Hasegawa, T.; Fukumura, T.; Kawasaki, M.; Ahmet, P.; Chikyow, T.; Koshihara, S.; Koinuma, H. *Science* **2001**, *291*, 854. Ando, K.; Saito, H.; Jin, Z.; Fukumura, T.; Kawasaki, M.; Matsumoto, Y.; Koinuma, H. *J. Appl. Phys.* **2001**, *89*, 7284. Ohno, Y.; Young, D. K.; Beschoten, B.; Matsukura, F.; Ohno, H.; Awschalom, D. D. *Nature* **1999**, *402*, 790. Fiederling, R.; Keim, M.; Reuscher, G.; Ossau, W.; Schmidt, G.; Waag, A.; Molenkamp, L. W. *Nature* **1999**, *402*, 787. Kossut, J. *Acta Phys. Pol. A* **2001**, *100*, 111.
- (9) Ueda, K.; Tabata, H.; Kawai, T. *App. Phys. Lett.* **2001**, *79*, 988. Ando, K.; Saito, H.; Jin, Z.; Fukumura, T.; Kawasaki, M.; Matsumoto, Y.; Koinuma, H. *App. Phys. Lett.* **2001**, *78*, 2700.
- (10) Radovanovic, P. V.; Gamelin, D. R. *J. Am. Chem. Soc.* **2001**, *123*, 12207.
- (11) Levy, L.; Feltin, N.; Ingert, D.; Pileni, M.-P. *Langmuir* **1999**, *15*, 3386. Norris, D. J.; Yao, N.; Charnock, F. T.; Kennedy, T. A. *Nano Lett.* **2001**, *1*, 3. Hoffman, D. M.; Meyer, B. K.; Ekimov, A. I.; Merkulov, I. A.; Efros, A. L.; Rosen, M.; Cunnio, G.; Gacoin, T.; Boilot, J.-P. *Solid State Commun.* **2000**, *114*, 547. Bol, A. A.; Meijerink, A. *Phys. Rev. B* **1998**, *58*, 15997. Suyver, J. F.; Wuister, S. F.; Kelly, J. J.; Meijerink, A. *Phys. Chem. Chem. Phys.* **2000**, *2*, 5445.
- (12) Mikulec, F. V.; Kuno, M.; Bennati, M.; Hall, D. A.; Griffin, R. G.; Bawendi, M. G. *J. Am. Chem. Soc.* **2000**, *122*, 2532.
- (13) Look, D. C. *Mater. Sci. Eng.* **2001**, *B80*, 383.
- (14) In a typical preparation, $\text{TM}^{2+}:\text{ZnO}$ QDs were synthesized by stirring 50 mL of 0.15 M LiOH into 50 mL of 0.1 M $\text{Zn}(\text{OAc})_2 \cdot 2\text{H}_2\text{O}$ and 0.005 M $\text{TM}(\text{OAc})_2 \cdot 4\text{H}_2\text{O}$ in EtOH at 0°C , allowing growth at 25°C for several days. The resulting nanocrystals were washed by repeated precipitation with heptane and resuspension in EtOH to form clear colloid solutions. Absorption data were collected using a Cary 5E spectrophotometer. Nanocrystal diameters were estimated from band gap energies.¹⁵ Co^{2+} concentrations ($\pm 10\%$) were determined by atomic emission spectrometry, and Ni^{2+} concentrations ($\pm 20\%$) were estimated from literature absorption coefficients.¹⁷ Highly crystalline wurzite ZnO was confirmed by powder XRD and TEM (Supporting Information).
- (15) Pesika, N. S.; Hu, Z.; Stebe, K. J.; Searson, P. C. *J. Phys. Chem. B* **2002**, *106*, 6985. Meulenkamp, E. A. *J. Phys. Chem. B* **1998**, *102*, 5566.
- (16) Cotton, F. A.; Goodgame, D. M. L.; Goodgame, M. *J. Am. Chem. Soc.* **1961**, *83*, 4690.
- (17) Weakliem, H. A. *J. Chem. Phys.* **1962**, *36*, 2117.

JA028416V